CONF-9411152--6

UCRL-JC-117302
PREPRINT

Diode-Pumped Solid State Laser for Inertial Fusion Energy

S. A. Payne
W. F. Krupke
C. D. Orth
C. D. Marshall
M. A. Emanuel

This paper was prepared for submittal to the International Atomic Energy Agency
Technical Committee Meeting on Drivers for Inertial Confinement Fusion
Paris, France
November 14–18, 1994

November 1994

Lawrence Livermore National Laboratory

DISCLAIMER

Diode-Pumped Solid State Laser for Inertial Fusion Energy

Stephen A. Payne, William F. Krupke, Charles D. Orth,
Christopher D. Marshall, and Mark A. Emanuel

Lawrence Livermore National Laboratory
Livermore, CA 94550 USA

Abstract

We evaluate the prospect for development of a diode-pumped solid-state-laser driver in an inertial fusion energy power plant. Using a computer code, we predict that our 1 GWe design will offer electricity at 8.6 ¢/kW · hr with the laser operating at 8.6% efficiency and the recycled power level at 31%. The results of our initial subscale experimental testbed of a diode-pumped solid state laser are encouraging, demonstrating good efficiencies and robustness.

I. Introduction

In the past it had been thought that solid-state lasers could not offer adequate efficiency, cost, repetition rate, or reliability to serve as the driver in an inertial fusion energy (IFE) power plant. Although Nd:glass solid-state lasers have provided the main means by which the physics of inertial confinement fusion (ICF) have been elucidated,[1] several technology innovations are required in order to enhance the performance of such lasers to render solid-state lasers suitable for IFE. In particular, we suggest the following four enhancements to flashlamp-pumped Nd:glass lasers : (1) The flashlamp pump sources must be replaced by laser diodes to increase the efficiency and reliability. (2) Forced turbulent cooling must be used to conduct heat out of the laser slabs by rapidly flowing helium across the optical apertures. (3) The Nd:glass gain medium must be replaced with an improved laser material possessing a longer storage time. (4) The debris shields must be replaced with heated fused-silica final optics in order to rapidly anneal out the neutron-induced color-center defects. With these new technologies it appears possible to design and construct a diode-pumped solid-state laser (DPSSL) with cost and performance adequate for IFE. The characteristics and performance of a DPSSL operating within the context of a 1 GWe power plant are described herein.

II. Laser Components

A. Laser diodes. The main issues surrounding the laser diode pump sources are the attainable efficiency, cost, and reliability. While efficiencies of >60% have been achieved, diodes typically exhibit "burn-in" behavior where the output is diminished somewhat. We have chosen to use 55% efficiency as the average value for a 30 year plant lifetime. Although the total number of laser pulses will need to be on the order of 10^{10} shots, $>10^9$ shots have already been demonstrated; it is therefore reasonable to suggest that research activities will lead to diodes that function for the duration of plant operations.

The cost of the laser diodes figures prominently in the total cost of the power plant. While we are unable to accurately predict the diode cost 20-30 years into the future, we can examine present trends for guidance. In Fig. 1 we plot LLNL-based experience in diode cost against the year, where we have assumed that low-duty-cycle diodes are employed and that the annual market is 3 MW/yr; here we have included direct labor, benefits, materials, and process yield, while excluding overhead, marketing, equipment, depreciation, and profit. These cost data reveal a compelling case for future decreases in diode cost. Further examination of cost centers indicates that the present rack-and-stack technology[5] will scale to about $0.50/watt at several MW/yr production, although less labor-intensive diode structures such as a 2D monolithic architecture should scale to costs as low as 3¢/watt. We employ a price of 7¢/watt in our calculations, and regard this cost objective as a rational goal.

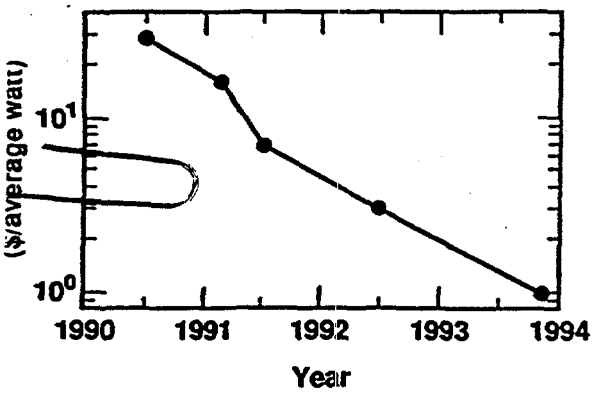

Fig. 1. LLNL diode cost plotted against year (see text for assumptions).

B. Laser gain medium. The laser requirements of IFE are somewhat unique in that the repetition rate is limited to below about 20 Hz (due to the operation of the fusion chamber), although the energy per pulse must be high. This scenario, and the high cost of diode pump sources, compels the designer to employ laser gain media characterized by long storage times. The most common laser materials are based on the Nd laser ion, since it possesses a suitable pump band and gain cross section. On the other hand, the Nd storage time tends to be too low. After consideration of the potential alternative laser ions, Yb was selected as the most promising candidate.

The plot in Fig. 2 contains the storage times and gain cross sections characterizing numerous Yb and Nd-doped materials where the data corresponding to each type of host material is connected with a line.[5,6] From this figure it becomes clear that, for a given host medium, Yb offers a 3-5× longer lifetime than Nd. It is also apparent that the Yb-doped media have much lower gain cross sections. After consideration of many issues, we have concluded that Yb:$Sr_5(PO_4)_3F$ (Yb:S-FAP) offers the best overall combination of optical, thermomechanical, and crystal growth properties.

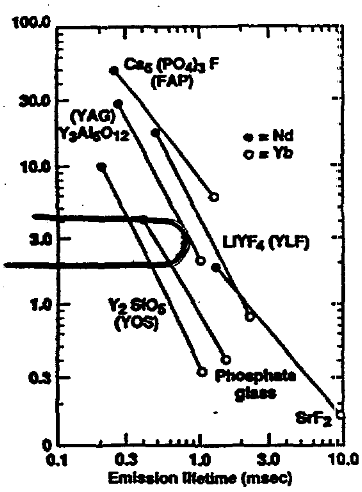

Fig. 2. Comparison of storage times and gain cross section for materials doped with Nd and with Yb.

C. Heated fused-silica final optic. One of the crucial issues confronting any type of laser driver for IFE is that the so-called "final optic" must survive the fluence of neutrons emanating from the target. A conceptual solution to this problem has been proposed where the fused-silica optic is held at about 400°C in order to rapidly anneal out the defects that are induced by the neutrons.[7] The data shown in Fig. 3 illustrate how the UV absorption can be diminished by heating the material. The kinetics of the defect formation and annealing have been included in our system-level analysis of the DPSSL IFE problem.

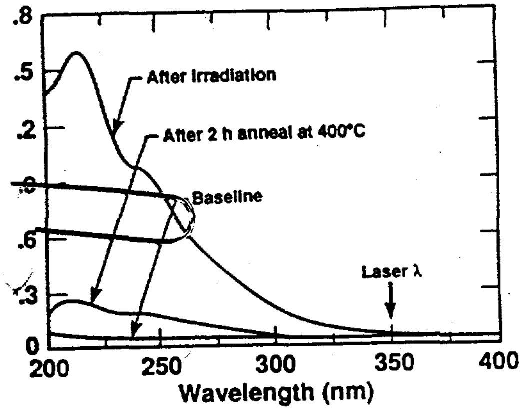

Fig. 3. UV absorption induced by neutrons in fused silica, and evidence of annealing behavior.

D. Gas-cooled slab. Most solid-state laser systems are cooled by water, although some involve conductive cooling into a solid medium. Neither of these approaches seems to be adaptable to the fusion laser architecture, where both heat and laser light are transmitted through the same surface of the slab. Here we envision the use of helium gas-cooling across the optical aperture of the gain medium slabs. The gas-cooling technique transforms the thermal distortions into a simple beam-steering effect, which is easily corrected. A series of papers on gas-cooling has appeared in the scientific literature, where a detailed mathematical description with experimental verification has been reported.[8] This detailed description of gas-cooling has been included in our IFE computer model. The 0.74 cm thick Yb:S-FAP slabs in our baseline design require a He flow rate at 0.067 Mach in a 3.6 mm channel in order to remove 0.75 W/cm^2 of heat from the surface. Under these conditions the thickness-averaged slab temperature turns out to be 57°C. The gas-cooling techniques are also required for other optical components such as the Pockels cells and the frequency-mixing crystals.

III. System Design

A. Laser architecture. The layout of a beamlet is sketched in Fig. 4, showing that the multipass (4×) amplifier resembles Beamlet at LLNL[9] and that the laser diodes are configured to longitudinally pump the 11 gas-cooled Yb:S-FAP slabs on each end of the amplifier. The Pockels cell/polarizer is used to switch-out the pulse, which is frequency-tripled prior to encountering the fused silica wedges serving as the final optics. The second fused silica wedge incurs the neutron yield and is therefore held at 400°C to anneal out the color center defects. The system design calls for 345 beamlines to produce 3.7 MJ of light for driving the target hohlraum, as required by our baseline 1 GWe power plant.

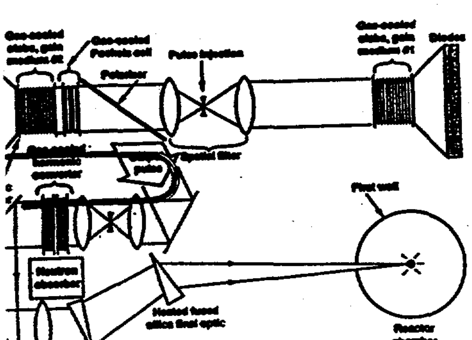

Fig. 4. Layout of single beamline.

Each slab is segmented transversely into 15 "subslabs" to mitigate the pumping losses associated with amplified spontaneous emission (ASE). Every subslab experiences a thermal transition region along its perimeter (which is on the order of one-half its thickness), where the optical distortions exclude focusability into the target. The resulting fill-factor loss is taken into account in our modeling.

B. Pumping and extraction calculations. Our DPSSL IFE model solves the differential equations governing the pumping of the Yb:S-FAP gain medium with laser diode arrays. The pie chart in Fig. 5 illustrates how the pump energy is apportioned among the various processes.

The largest loss is due to simple emission, although smaller contributions from ASE and pump transmission also occur, yielding a 60% pump efficiency for the 1 GWe baseline design.

The extraction efficiency of Yb:S-FAP is calculated to be 70% (excluding the fill factor). Figure 6 shows how the initial profiles along the longitudinal axis of the amplifier are modified after four passes of the input pulse. This calculation takes the passive losses into account (0.05-0.5%/cm, depending on the optic), as well as the surface reflections.

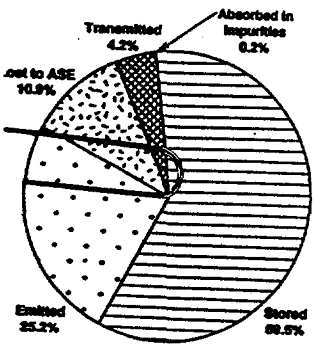

Fig. 5. Pie chart of pump power use.

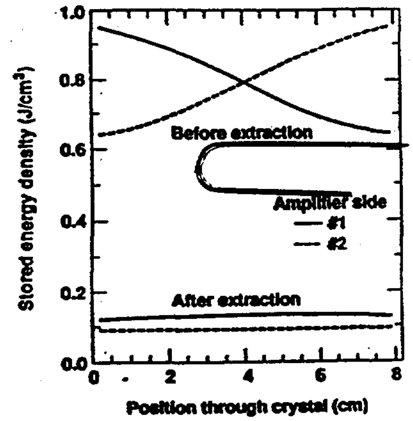

Fig. 6. Initial and final Yb excited state profiles along longitudinal axis of the amplifier.

C. Fusion gain curve and beam quality. Our model is based on the indirect drive gain curve labeled baseline in Fig. 7. One of the crucial parameters is the size d_{LEH} of the laser entrance hole (LEH), which is given as:

$$d_{LEH} = f_{bo} \cdot d_o \left[\frac{E_{3\omega}\,\eta_{cp}}{1\ \mathrm{MJ}}\right]^{0.56}$$

where $f_{bo} = 0.8$ is the blow-off factor leading to hole closure, $d_o = 0.45$ cm, $E_{3\omega}$ is the third harmonic energy of the laser, and η_{cp} is the target coupling of 0.11-0.20 (depending on the laser energy). The beam quality issue is treated by assuming that each optic or subslab imposes $\lambda/30$ distortion onto the laser beam, and that the light must be focused into the LEH in order to participate in generating fusion.

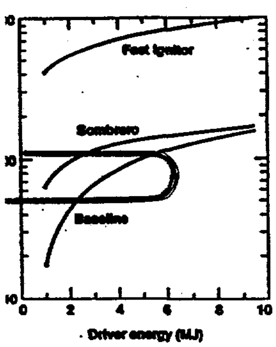

Fig. 7. Fusion gain curve used in 1 GWe system study (based on indirect drive).

D. Balance-of-plant and costs. The balance-of-plant costs and efficiencies were used directly from the Sombrero report in the literature[10] including the fusion chamber, steam turbines, heat exchangers, etc. The laser costs were estimated for the 20-30 year future time frame in a laser fusion economy (e.g., optical finishing at \$1/cm² and front end at \$15k/joule).

E. Optimization and laser performance. Our computer model adjusts the laser architecture in order to minimize the COE, including the diode pump time, repetition rate, pump absorption, Yb concentration, amount of ASE, and size of each subslab (see Fig. 8). After iterative consideration of these variables, the COE becomes 8.6¢/kW · hr.

Fig. 8. Plots showing optimization of laser variables.

The bar graph in Fig. 9 illustrates the cumulative impact of numerous effects leading to the overall laser efficiency of 8.6%. The pump and diode efficiencies are most significant, although other issues (such as the cooling) combine to have an important impact. It is noteworthy that the laser efficiency of 8.6% is a consequence of minimizing the COE — not maximizing the laser efficiency. If costs were not explicitly included, the laser efficiency could reach about 15%.

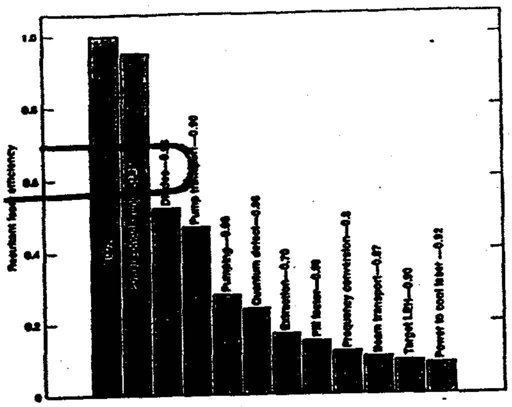

Fig. 9. Individual efficiencies impacting laser driver.

F. Power plant cost and performance. Fig. 10 indicates the distribution of system costs. Interestingly, the laser diodes represent 75% of the laser cost, while the laser is 41% of the total power plant cost. The flow of power is depicted in Fig. 11, where it is seen that the recycled power is 32% of the electrical output. Although this fraction is larger than is preferable, it nevertheless represents a situation that appears workable.

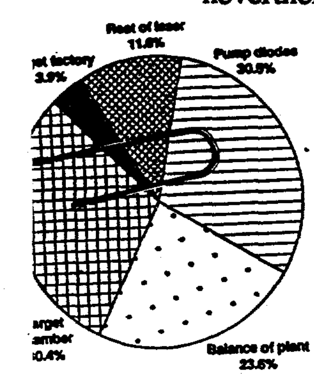

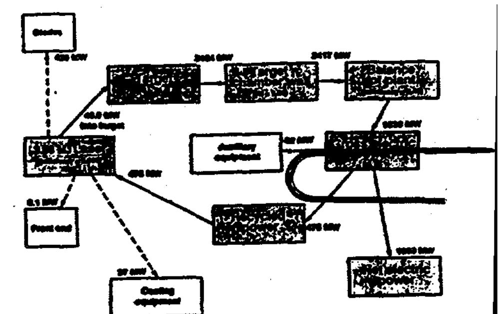

Fig. 10. Breakout of system costs.

Fig. 11. Flow of power in system.

Several avenues for improvement over our baseline design also exist. As shown in Fig. 12, diode prices below 7¢/watt would be advantageous, as would the discovery of a new gain medium having a longer storage time (while retaining the otherwise favorable features of Yb:S-FAP). Most significant, however, would be enhancements in the target gain. Lastly, fusion power plants employing liquid walls could increase the plant availability toward 90%.[11]

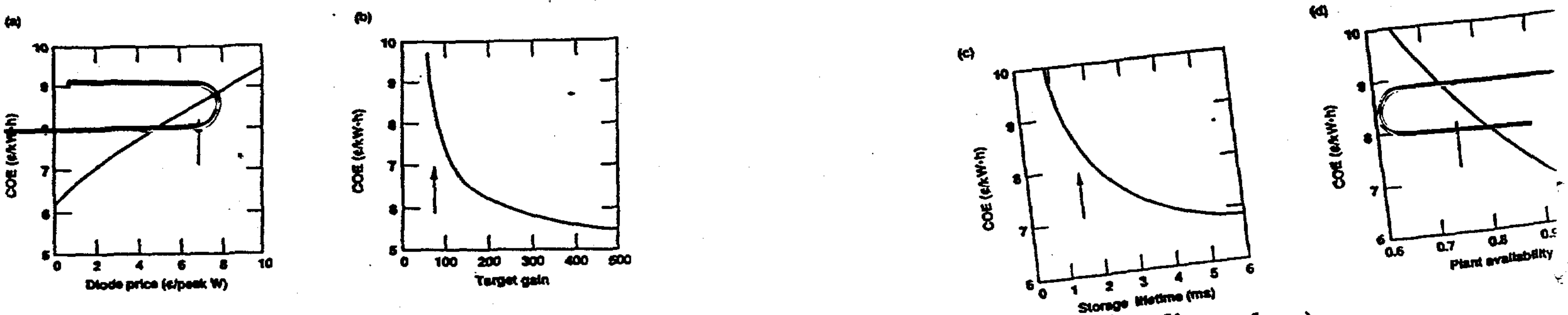

Fig. 12. High leverage areas for improvement (arrow denotes baseline values).

III. Yb:S-FAP DPSSL Demonstration

We have measured the 1.047 μm small-signal gain evidenced from an Yb:S-FAP crystal pumped at 0.90 μm.[3,5,6] The data in Fig. 13 indicate that the gain cross section is 6.0×10^{-20} cm^2, which is close to the spectroscopically-derived value of 7.3×10^{-20} cm^2. Furthermore, we have constructed a small DPSSL and obtained encouraging initial results. We have also fabricated an InGaAs laser diode array and achieved 40% efficiency. The resulting Yb:S-FAP DPSSL slope efficiency of 9.1% is displayed in Fig. 14. While this laser is operated in a quasi-continuous long-pulse mode (in contrast to the energy storage mode required for IFE), these results are encouraging. The Yb:S-FAP crystals have low scattering loss (<0.1%/cm), although impurities currently induce an absorptive loss of about 1%/cm. The recently discovered Yb:S-FAP laser crystal thus appears to be viable even at this very early stage of development.

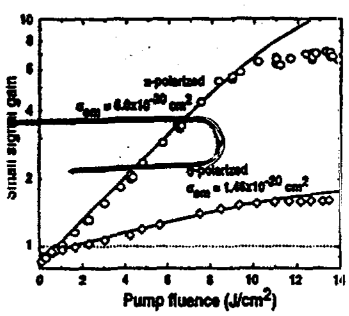

Fig. 13. Gain observed for Yb:S-FAP crystal.

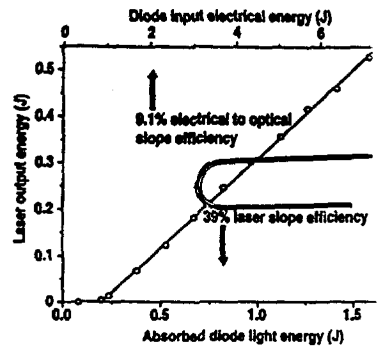

Fig. 14. Efficiency of Yb:S-FAP DPSSL.

IV. Conclusions

Our conceptual approach and initial experiments suggest that the DPSSL is a viable driver candidate for IFE. The DPSSL driver strategy has several important advantages: (1) It is based on the well-known physics of fusion lasers; (2) DPSSL architecture is inherently modular in nature; and (3) DPSSL technology is advancing independently on a parallel path involving industrial-commercial-military applications. These aspects of the DPSSL driver are likely to reduce risk and lead to lower development costs.

Acknowledgments

We are happy to thank many people throughout the Laser Programs at LLNL for their guidance and advice. This work was performed under the auspices of the U.S. Department of Energy by Lawrence Livermore National Laboratory under Contract No. W-7405-ENG-48.

References

1. For example, see E. M. Campbell, Phys. Fluids B 4, 3781 (1992).
2. C. D. Orth, S. A. Payne, and W. F. Krupke, "A diode-pumped solid-state laser driver for inertial fusion energy," submitted to Nuclear Fusion in September 1994.
3. C. D. Marshall, S. A. Payne, L. K. Smith, H. T. Powell, W. F. Krupke, and B. H. T. Chai, "1.047 μm Yb:$Sr_5(PO_4)_3F$ energy storage optical amplifier," submitted to IEEE J. Quantum Electronics in September 1994.
4. R. Beach, W. Benett, B. Freitas, D. Mundinger, B. Comaskey, R. Solarz, and M. Emanuel, IEEE J. Quantum Electron. 28, 966 (1992).
5. L. D. DeLoach, S. A. Payne, L. K. Smith, W. L. Kway, and W. F. Krupke, J. Opt. Soc. Am. B 11, 269 (1994)
6. S. A. Payne, L. D. DeLoach, L. K. Smith, W. L. Kway, J. B. Tassano, W. F. Krupke, B. H. T. Chai, and G. Loutts, J. Appl. Phys. 76, 497 (1994).

7. J. G. Woodworth, L. L. Chase, M. W. Guinan, W. F. Krupke, and W. R. Sooy, The 14th IEEE/NPSS Symposium on Fusion Engineering (San Diego, CA, September 30-October 3, 1991).
8. S. B. Sutton and G. F. Albrecht, J. Appl. Phys. 69, 1183 (1991).
9. B. M. van Wonterghem, J. R. Murray, D. R. Speck, and J. H. Campbell, 11th Topical Meeting on the Technology of Fusion Energy (New Orleans, LA) June 19-23, 1994).
10. W. R. Meier and C. W. van Rosenberg, Jr., Fusion Technology 21, 1552 (1992).
11. R. W. Moir, R. L. Bieri, X. M. Chen, T. J. Dolan et al., Fusion Tech. 25, 5 (1994).